Molecular Imaging

DOI: 10.1002/ange.201400428

DNA-Templated Assembly of a Heterobivalent Quantum Dot Nanoprobe For Extra- and Intracellular Dual-Targeting and Imaging of Live Cancer Cells**

*Wei Wei, Xuewen He, and Nan Ma**

Abstract: *Quantum dots (QDs) hold great promise for the molecular imaging of cancer because of their superior optical properties. Although cell-surface biomarkers can be readily imaged with QDs, non-invasive live-cell imaging of critical intracellular cancer markers with QDs is a great challenge because of the difficulties in the automatic delivery of QD probes to the cytosol and the ambiguity of intracellular targeting signals. Herein, we report a new type of DNA-templated heterobivalent QD nanoprobes with the ability to target and image two spatially isolated cancer markers (nucleolin and mRNA) present on the cell surface and in the cell cytosol. Bypassing endolysosomal sequestration, this type of QD nanoprobes undergo macropinocytosis following the nucleolin targeting and then translocate to the cytosol for mRNA targeting. Fluorescence resonance energy transfer (FRET) based confocal microscopy enables unambiguous signal deconvolution of mRNA-targeted QD nanoprobes inside cancer cells.*

Molecular imaging has emerged as an important technique over the past decade for cancer detection, personalized treatment, drug development, and elucidation of the origin of cancer.[1] Quantum dots (QDs) could offer great promise as a class of superior luminophores for the molecular imaging of cancer because of their strong photoluminescence, high photostability, and unique size-dependent optical properties.[2] Despite the progress that has been made toward the imaging of cancer markers present on the cell surface with QDs, live-cell imaging of critical intracellular tumor-associated biomolecules using QDs is of great interest but still remains problematic. Firstly, the cellular uptake of QDs predominantly results in endolysosomal sequestration of QDs that are not accessible for biomolecular targeting inside the cells.[3] Capping QDs with endosome-disrupting polymers could enable the cytosolic delivery of QDs, but is extremely destructive to live cells.[4] Liposome and cell-penetrating peptide-aided delivery of QDs could cause severe aggregation and lysosomal sequestration of the QDs.[3e,5] Microinjection-based delivery of QDs is low-throughput and invasive, thus limiting their use for molecular imaging. To date, non-invasive cytosolic delivery of QDs mainly relies on large biodegradable nanocomposites or special peptides.[6] Additionally, isolating the signals of intracellular targeted QDs from free QDs remains impractical because of the lack of efficient methods to clear free QDs from inside the live cells. Therefore, the targeted imaging of intracellular biomolecules necessitates both the automatic cytosolic delivery of QD probes and an optical signal response to the specific targeting event, which has not been previously accomplished.

Aside from its extraordinary self-assembly properties, DNA has proven to be highly versatile for biomolecular targeting.[7] Various types of biomolecules, including nucleic acids, proteins, cell-surface receptors, and small molecules, can be targeted by DNA aptamers with high affinity and specificity.[8] On the other hand, DNA can serve as a unique template for the synthesis of QDs.[9] DNA-capped QDs possess high stability, small hydrodynamic sizes, minimal nonspecific binding, and low toxicity to various cell types.[10] In addition, the DNA-templated synthesis of QDs by using hybrid DNA molecules with phosphorothioate linkages yields DNA-functionalized QDs with precisely controlled DNA valencies, thus enabling the construction of higher-order QD-based nanostructures with well-defined geometries through DNA hybridization.[10,11]

Herein we report a new type of DNA-templated heterobivalent QD nanoprobe with dual extracellular and intracellular targeting and imaging capabilities of cancer markers. We designed a hybrid DNA template containing a phosphorothioate domain in the center (Figure 1, purple) for growth of the QD and two phosphate domains at each end (blue and orange) for the assembly of two cancer-targeting motifs—an extracellular nucleolin-targeting motif (NTM) and an intracellular mRNA-targeting motif (MTM). Since Cd^{2+} ions exhibit a 3000-fold preference for sulfur over oxygen binding when presented with nucleotides, the phosphorothioate domain would tightly bind to the surface of a cadmium-based QD and the two phosphate domains would remain unbound and free to hybridize with other DNA molecules.[10,11] AS1411, a nucleolin-binding aptamer, was selected for the extracellular targeting of cancer cells because nucleolin is overexpressed on most types of cancer cells but not on normal cells, and the aptamer could stimulate macropinocytosis in cancer cells.[12] By targeting nucleolin on the cell

[*] W. Wei, X. He, Prof. N. Ma
The Key Lab of Health Chemistry and Molecular Diagnosis of Suzhou
College of Chemistry, Chemical Engineering and Materials Science
Soochow University, Suzhou, 215123 (P.R. China)
E-mail: nan.ma@suda.edu.cn
Homepage: http://maresearchgroup.net

[**] This work was supported in part by the National Natural Science Foundation of China (21175147, 91313302), the National High-Tech R&D Program (863 program) (2014AA020518), the Recruitment Program of Global Young Experts (1000-Young Talents Plan), the Project of Scientific and Technologic Infrastructure of Suzhou (SZS201207), and startup funds from Soochow University.

Supporting information for this article is available on the WWW under http://dx.doi.org/10.1002/anie.201400428.

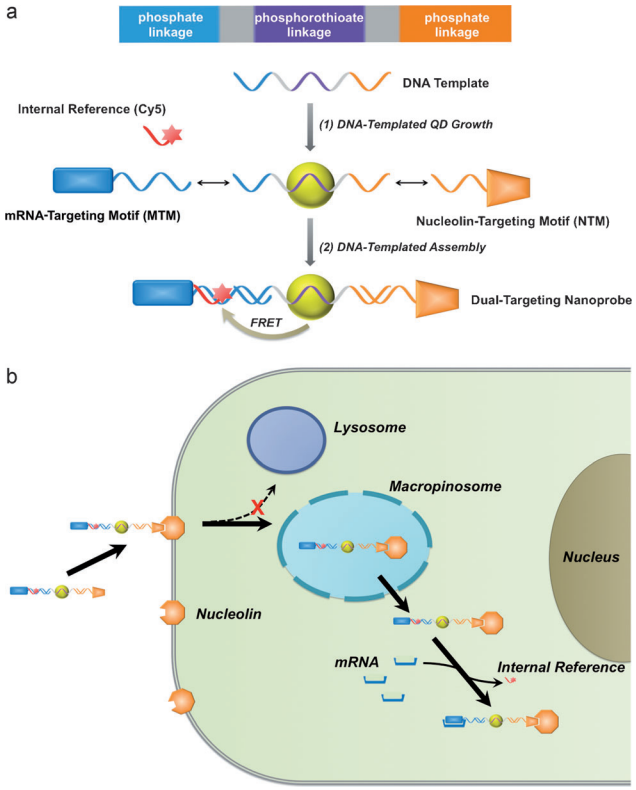

Figure 1. Schematic illustration of a) the construction of a DNA-templated heterobivalent QD nanoprobe; b) the dual-targeting strategy and intracellular delivery route of the heterobivalent QD nanoprobe.

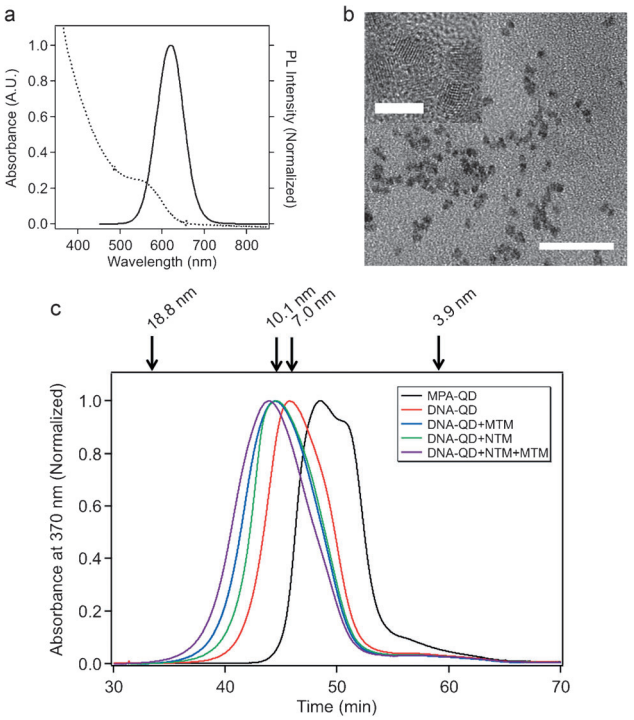

Figure 2. Synthesis and assembly of DNA-capped CdTe QDs. a) Representative absorption and photoluminescence (PL) spectra of DNA-capped CdTe QDs. b) Low magnification and high-resolution (inset) TEM images of DNA-capped CdTe QDs. (Scale bars are 50 nm and 5 nm, respectively.) c) GFC characterization of the assembly of DNA-capped QDs with NTM and MTM. QDs synthesized with MPA alone are used as a control. Positions of protein standards with known HD sizes are indicated at the top of the graph.

surface, the QD nanoprobe could undergo efficient macropinocytosis and localize in macropinosomes. Subsequently, the QD nanoprobe could escape from the leaky macropinosomes and translocate to the cytosol for intracellular mRNA targeting (Figure 1b). Tumor-associated mRNA is an important type of intracellular marker for cancer detection.[13] The MTM is a 20-mer antisense DNA complementary to survivin mRNA that is highly up-regulated in HeLa cells.[14] This antisense DNA is known to down-regulate survivin mRNA through an RNase H dependent mechanism.[14c] To create an optical signal response for mRNA targeting, a Cy5-labeled oligomer (internal reference) was assembled onto the MTM to generate fluorescence resonance energy transfer (FRET) between the QD and Cy5. Binding of MTM with the longer mRNA target will release the internal reference and switch off the FRET signal, which can be monitored by confocal microscopy and colocalization studies. Moreover, phosphorothioate linkers are incorporated into the MTM to minimize enzymatic degradation of the probe.

The heterobivalent QD nanoprobe was constructed in two steps. Firstly, DNA-capped CdTe QDs were synthesized according to a previously reported procedure.[11] Typical absorption and emission spectra of the as-prepared DNA-capped QDs are illustrated in Figure 2a. The quantum yield (QY) of these QDs is 17.8%. The nanocrystalline QDs are nearly monodisperse with a mean diameter of 4.8 nm, as shown by TEM analysis (Figure 1b). Secondly, two targeting motifs (NTM and MTM) were assembled onto the DNA-capped QDs through hybridization between the phosphate domain of the DNA template and the complementary single-stranded DNA of the targeting motif. The assembly was monitored using gel filtration chromatography (GFC). The DNA-capped CdTe QDs exhibit an elution peak at 45.8 min (Figure 2c), which corresponds to a mean hydrodynamic (HD) size of 7.0 nm. Assembly of one and two targeting motifs onto the DNA-capped QDs results in a stepwise shift to a shorter elution time (44.5 min and 43.9 min) as a result of increased HD sizes. Next, a Cy5-labeled short oligomer was assembled onto a portion of the MTM through hybridization to give rise to FRET between QD and Cy5. The FRET efficiency is highly dependent on the QD emission wavelength. The FRET efficiency significantly increases as the QDs emission shifts from 570 to 640 nm because the emission band of the QDs at 640 nm has the most overlap with the absorption spectrum of Cy5 (Figure 3). The QDs with an emission maximum of 610 nm were used for further studies because they could provide both well-resolved emission bands of QDs and Cy5 as well as adequate FRET efficiency. The spectral overlap integral $J(\lambda)$, Förster distance R_0, and separation distance r of the QD (610 nm)/Cy5 FRET pair are calculated to be 1.84×10^{-12} cm^3 M^{-1}, 62.8 Å, and 65.5 Å, respectively (see the Supporting Information for details). To determine the number of DNA molecules on each QD, a Cy5-labeled oligomer was titrated against the DNA-capped QDs

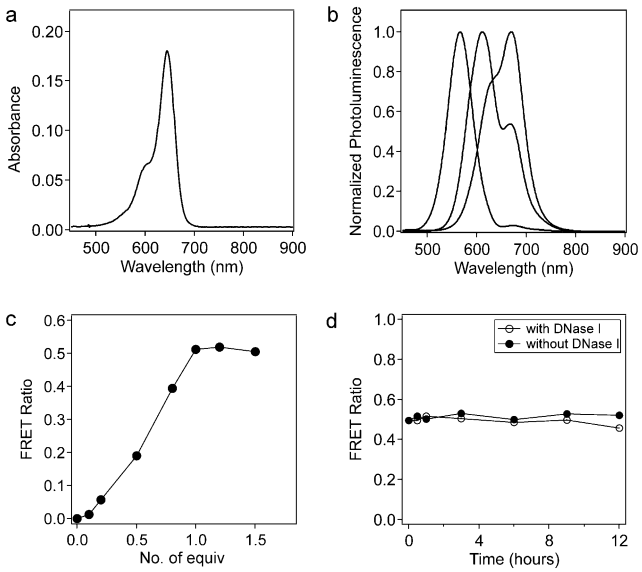

Figure 3. a) Absorption spectrum of Cy5-labeled oligomers. b) FRET spectra of QD nanoprobes assembled with Cy5-labeled oligomers. The molar ratio between MTM and Cy5-labeled oligomer is 1:1 for all the three QDs emitting at 570 nm, 610 nm, and 640 nm. The scaling factors for the three spectra (from left to right) are 7.3×10^{-5}, 1.1×10^{-4}, and 1.3×10^{-4}, respectively. c) FRET-based titration experiments for the determination of the average number of DNA molecules on each QD. d) Stability of QD nanoprobes treated with and without DNase I. The FRET ratio is recorded as a function of incubation time.

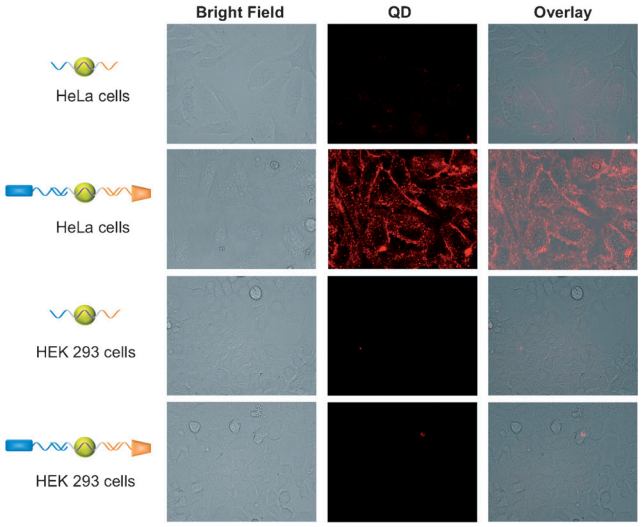

Figure 4. Confocal microscopy images of HeLa cells and HEK 293 cells incubated with the QD nanoprobe containing NTM and MTM at 37 °C for 1 h. DNA-capped QDs without NTM and MTM were used as controls.

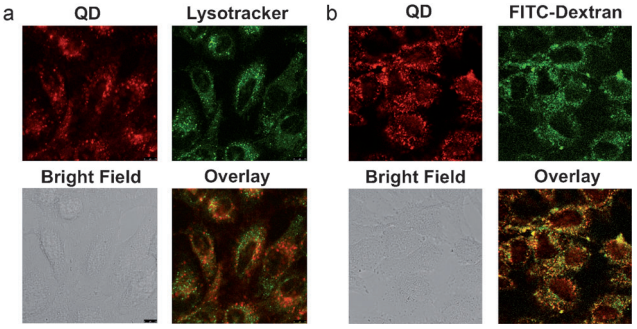

Figure 5. Colocalization of QD nanoprobes with LysoTracker Green DND-26 (a) and FITC-Dextran in HeLa cells (b).

and a plateau in the FRET efficiency was achieved at one equivalent of QDs. This result indicates that each QD is capped by one DNA template molecule on average, although some heterogeneity could exist.[15] These QD nanoprobes exhibit robust colloidal stability when incubated with cell media containing fetal bovine serum (FBS) at 37 °C for 24 h (see Figure S1 in the Supporting Information). The stability of the QD nanoprobe against nuclease (Dnase I) degradation was evaluated.[16] No apparent decrease in the FRET efficiency was observed during 12 h of incubation with Dnase I at 37 °C (Figure 3 d), which suggests that the QD nanoprobe is stable for intracellular experiments.

To explore the extracellular targeting capability of the QD nanoprobe, a nucleolin-overexpressing cancer cell line (HeLa cells) and a control cell line (HEK 293 cells) were incubated with the QD nanoprobe for 1 h at 37 °C, and the binding of the QDs with the cells was monitored using confocal microscopy. The QD nanoprobe specifically bound to the HeLa cells but not the HEK 293 cells (Figure 4). HeLa and HEK 293 cells incubated with the QDs without NTM or with a scrambled double-stranded NTM did not exhibit QD binding (see Figure S2 in the Supporting Information), thus confirming that the binding between the HeLa cells and the QD nanoprobe is a result of nucleolin targeting. These binding trends were further confirmed by flow cytometry (see Figure S3 in the Supporting Information). The intracellular localization of the QD nanoprobe was explored by colocalization with LysoTracker Green DND-26—a marker for late endosomes and lysosomes (Figure 5 a) and FITC-Dextran—a marker for macropinosomes (Figure 5 b). The Pearson's coefficients of the overlay images in Figure 5 a,b are −0.1 and 0.6, respectively, which reveals that the QDs were internalized by macropinocytosis. Macropinosomes are more leaky than other endosomal vesicles and their cargo could bypass degradative processing and escape from macropinosomes.[17] When the incubation time was increased from 1 to 4 h, more QDs were internalized into the HeLa cells and exhibited a homogeneous, diffusive, and delocalized pattern as a result of cytosolic delivery (Figure 6). A high-degree of colocalization between the QDs and a cytoplasmic tracker—Calcein AM—was observed, thus confirming the cellular uptake of the QDs (see Figure S4 in the Supporting Information). This result is distinct from perinuclear endolysosomal confinement of QDs internalized through the regular endocytic pathway.[3]

Based on the above results, we envision that these QD nanoprobes could be applied to the imaging of intracellular biomolecular targets. To monitor mRNA targeting, the QD signal (green color) and the Cy5 FRET signal (red color) were recorded with the same excitation (405 nm) but different emission filter sets. The overlay image of the QD signal and the Cy5 FRET signal could distinguish between the mRNA-

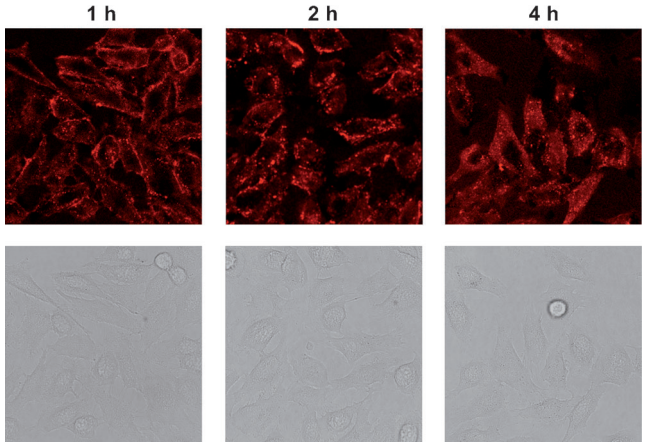

Figure 6. Incubation time dependence of cellular localization of QD nanoprobes. Confocal microscopy images of HeLa cells incubated with QD nanoprobes for 1, 2, and 4 h.

targeted QD nanoprobe (green color) and the original QD nanoprobe (yellow color). In addition, the release of Cy5-labeled oligomers can be monitored through colocalization between the QD signal and the directly excited Cy5 signal. After 1 h incubation with the QD nanoprobe, the HeLa cells exhibited a nearly complete overlap of the QD photoluminescence signal and the Cy5 FRET signal (Figure 7a), which suggests that mRNA targeting had not occurred. A high-degree of colocalization between the QD signal and the directly excited Cy5 signal was also observed (Figure 7a), thus suggesting that most of the Cy5-labeled oligomer remained associated with the nanoprobe. When the incubation time was increased to 4 h, a pronounced decrease of the FRET signal inside the cells was evident, whereas the FRET signal close to the cell surface remained unaffected (Figure 7b). The overlay image of the QD signal and the Cy5 FRET signal illustrates the predominance of the intracellular mRNA-targeted QD nanoprobes (depicted in green in Figure 7b). An overlay of the directly excited Cy5 signal and the QD signal in the cells reveals that a significant amount of Cy5-labeled oligomers was released from the QD nanoprobe in the cells (Figure 7b). About 90% of the cells examined in five randomly picked regions (150–250 cells) exhibited the same patterns as indicated in Figure 7. To further confirm the specificity of intracellular mRNA targeting, a QD nanoprobe containing a scrambled MTM was used as a control for the imaging studies. In stark contrast to the mRNA-targeting QD nanoprobe, the intracellular FRET signal of the control QDs was highly preserved in the HeLa cells after 4 h (Figure 7c). Furthermore, the overlay of the QD signal and the directly excited Cy5 signal reveals a high-degree of colocalization, which indicates that most Cy5 molecules remained associated with the QD nanoprobe. These results suggest that the QD nanoprobe is specific for intracellular mRNA imaging and is not susceptible to nonspecific binding or probe degradation. Cell viability was determined using the MTT (3-[4,5-dimethylthiazol-2-yl]-2,5 diphenyltetrazolium bromide) assay, and about 92% of the HeLa cells were alive after 4 h (see Figure S6 in the Supporting Information).

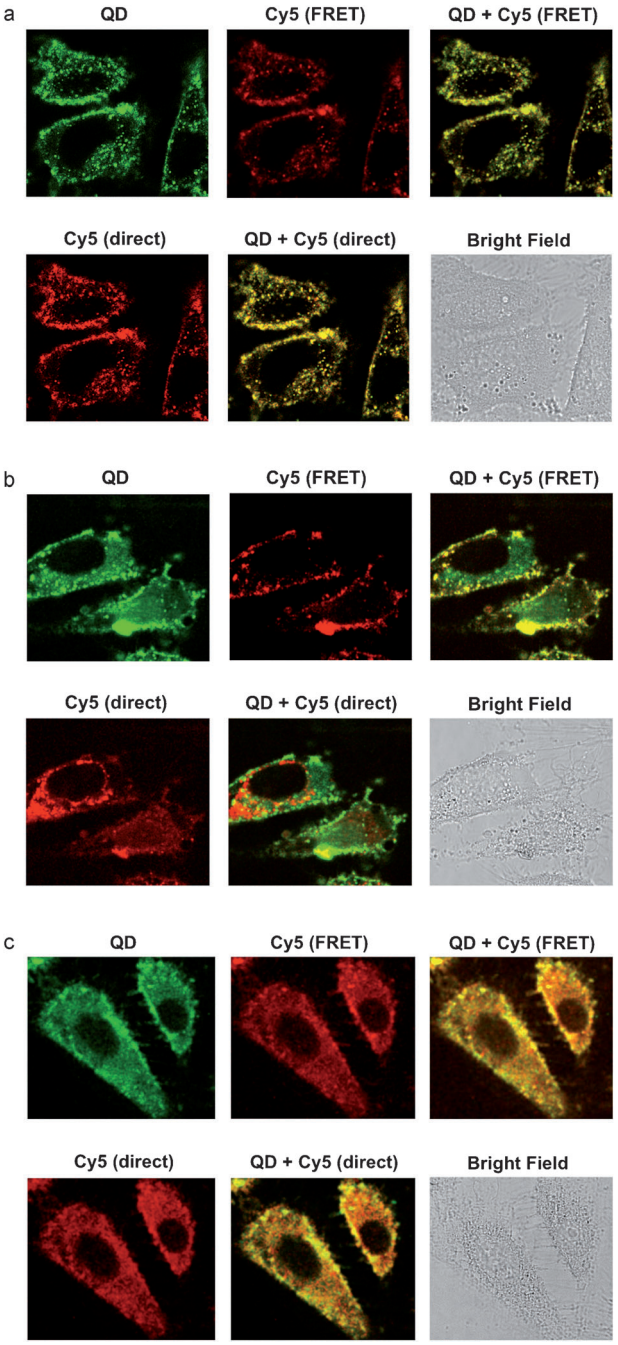

Figure 7. Intracellular survivin mRNA targeting and imaging using QD nanoprobes. Confocal microscopy images of HeLa cells incubated with mRNA-targeting QD nanoprobes for 1 h (a) and 4 h (b) and HeLa cells incubated with non-mRNA-targeting (scrambled MTM) QD nanoprobes for 4 h (c). Top panel (from left to right): QD signal image; Cy5 FRET signal image; overlay of QD signal and Cy5 FRET signal image. Bottom panel (from left to right): directly excited Cy5 signal image; overlay of QD signal and directly excited Cy5 signal image; bright field image.

In conclusion, we report a new type of DNA-templated heterobivalent QD nanoprobe featuring two targeting motifs for dual extracellular and intracellular targeting and imaging of cancer markers. We show that the targeting of cell-surface nucleolin by NTM facilitates macropinocytosis of the QD

nanoprobe and the subsequent cytosolic delivery of the nanoprobe for intracellular mRNA targeting. This type of QD nanoprobe could bypass the commonly existing lysosomal sequestration of QDs probes and achieve targeted imaging of intracellular biomolecules. This approach also opens up the possibility of elucidating the complex biological processes in cancer cells using QDs. Given the versatility of DNA aptamers for biomolecule targeting and the general aptamer beacon-based FRET reporters,[18] we expect that the reported QD nanoprobe could serve as a general tool for the imaging of a variety of intracellular biomolecules in cancer cells.

Received: January 15, 2014
Revised: March 13, 2014
Published online: April 16, 2014

Keywords: cancer · DNA · imaging agents · mRNA · quantum dots

[1] R. Weissleder, *Science* **2006**, *312*, 1168 – 1171.
[2] a) X. Gao, Y. Cui, R. M. Levenson, L. W. K. Chung, S. Nie, *Nat. Biotechnol.* **2004**, *22*, 969 – 976; b) X. Wu, H. Liu, J. Liu, K. N. Haley, J. A. Treadway, J. P. Larson, N. Ge, F. Peale, M. P. Bruchez, *Nat. Biotechnol.* **2002**, *21*, 41 – 46; c) H. S. Choi, W. Liu, F. Liu, K. Nasr, P. Misra, M. G. Bawendi, J. V. Frangioni, *Nat. Nanotechnol.* **2010**, *5*, 42 – 47; d) X. Michalet, F. F. Pinaud, L. A. Bentolila, J. M. Tsay, S. Doose, J. J. Li, G. Sundaresan, A. M. Wu, S. S. Gambhir, S. Weiss, *Science* **2005**, *307*, 538 – 544; e) M. Green, *Angew. Chem.* **2004**, *116*, 4221 – 4223; *Angew. Chem. Int. Ed.* **2004**, *43*, 4129 – 4131; f) I. L. Medintz, H. Mattoussi, *Phys. Chem. Chem. Phys.* **2009**, *11*, 17 – 45.
[3] a) V. Biju, T. Itoh, M. Ishikawa, *Chem. Soc. Rev.* **2010**, *39*, 3031 – 3056; b) J. K. Jaiswal, H. Mattoussi, J. M. Mauro, S. M. Simon, *Nat. Biotechnol.* **2002**, *21*, 47 – 51; c) W. C. W. Chan, S. Nie, *Science* **1998**, *281*, 2016 – 2018; d) J. Xu, T. Teslaa, T.-H. Wu, P.-Y. Chiou, M. A. Teitell, S. Weiss, *Nano Lett.* **2012**, *12*, 5669 – 5672; e) J. B. Delehanty, C. E. Bradburne, K. Susumu, K. Boeneman, B. C. Mei, D. Farrell, J. B. Blanco-Canosa, P. E. Dawson, H. Mattoussi, I. L. Medintz, *J. Am. Chem. Soc.* **2011**, *133*, 10482 – 10489; f) J. Lee, A. Sharei, W. Y. Sim, A. Adamo, R. Langer, K. F. Jensen, M. G. Bawendi, *Nano Lett.* **2012**, *12*, 6322 – 6327.
[4] H. Duan, S. Nie, *J. Am. Chem. Soc.* **2007**, *129*, 3333 – 3338.
[5] a) A. M. Derfus, W. C. W. Chan, S. N. Bhatia, *Adv. Mater.* **2004**, *16*, 961 – 966; b) J. Silver, W. Ou, *Nano Lett.* **2005**, *5*, 1445 – 1449.
[6] a) B. Y. S. Kim, W. Jiang, J. Oreopoulos, C. M. Yip, J. T. Rutka, W. C. W. Chan, *Nano Lett.* **2008**, *8*, 3887 – 3892; b) K. Boeneman, J. B. Delehanty, J. B. Blanco-Canosa, K. Susumu, M. H. Stewart, E. Oh, A. L. Huston, G. Dawson, S. Ingale, R. Walters, M. Domowicz, J. R. Deschamps, W. R. Algar, S. DiMaggio, J. Manono, C. M. Spillmann, D. Thompson, T. L. Jennings, P. E. Dawson, I. L. Medintz, *ACS Nano* **2013**, *7*, 3778 – 3796.
[7] H. Xing, N. Y. Wong, Y. Xiang, Y. Lu, *Curr. Opin. Chem. Biol.* **2012**, *16*, 429 – 435.
[8] a) R. F. Macaya, P. Schultze, F. W. Smith, J. A. Roe, J. Feigon, *Proc. Natl. Acad. Sci. USA* **1993**, *90*, 3745 – 3749; b) D. E. Huizenga, J. W. Szostak, *Biochemistry* **1995**, *34*, 656 – 665; c) D. Shangguan, Y. Li, Z. Tang, Z. C. Cao, H. W. Chen, P. Mallikaratchy, K. Sefah, C. J. Yang, W. Tan, *Proc. Natl. Acad. Sci. USA* **2006**, *103*, 11838 – 11843.
[9] a) N. Ma, G. A. Tikhomirov, S. O. Kelley, *Acc. Chem. Res.* **2010**, *43*, 173 – 180; b) L. Gao, N. Ma, *ACS Nano* **2012**, *6*, 689 – 695; c) N. Ma, S. O. Kelley, *Wiley Interdiscip. Rev. Nanomed. Nanobiotechnol.* **2013**, *5*, 86 – 95; d) N. Ma, J. Yang, K. M. Stewart, S. O. Kelley, *Langmuir* **2007**, *23*, 12783 – 12787.
[10] N. Ma, E. H. Sargent, S. O. Kelley, *Nat. Nanotechnol.* **2009**, *4*, 121 – 125.
[11] G. Tikhomirov, S. Hoogland, P. E. Lee, A. Fischer, E. H. Sargent, S. O. Kelley, *Nat. Nanotechnol.* **2011**, *6*, 485 – 490.
[12] a) P. J. Bates, D. A. Laber, D. M. Miller, S. D. Thomas, J. O. Trent, *Exp. Mol. Pathol.* **2009**, *86*, 151 – 164; b) E. M. Reyes-Reyes, Y. Teng, P. J. Bates, *Cancer Res.* **2010**, *70*, 8617 – 8629.
[13] D. Sidransky, *Nat. Rev. Cancer* **2002**, *2*, 210 – 219.
[14] a) S. Fukuda, L. M. Pelus, *Mol. Cancer Ther.* **2006**, *5*, 1087 – 1098; b) R. A. Olie, A. P. Simões-Wüst, B. Baumann, S. H. Leech, D. Fabbro, R. A. Stahel, U. Zangemeister-Wittke, *Cancer Res.* **2000**, *60*, 2805 – 2809; c) N. M. Dean, C. F. Bennett, *Oncogene* **2003**, *22*, 9087 – 9096.
[15] T. Pons, I. L. Medintz, X. Wang, D. S. English, H. Mattoussi, *J. Am. Chem. Soc.* **2006**, *128*, 15324 – 15331.
[16] D. S. Seferos, A. E. Prigodich, D. A. Giljohann, P. C. Patel, C. A. Mirkin, *Nano Lett.* **2009**, *9*, 308 – 311.
[17] a) K. T. Love, K. P. Mahon, C. G. Levins, K. A. Whitehead, W. Querbes, J. R. Dorkin, J. Qin, W. Cantley, L. L. Qin, T. Racie, M. Frank-Kamenetsky, K. N. Yip, R. Alvarez, D. W. Y. Sah, A. de Fougerolles, K. Fitzgerald, V. Koteliansky, A. Akinc, R. Langer, D. G. Anderson, *Proc. Natl. Acad. Sci. USA* **2010**, *107*, 1864 – 1869; b) I. A. Khalil, K. Kogure, H. Akita, H. Harashima, *Pharmacol. Rev.* **2006**, *58*, 32 – 45.
[18] N. Hamaguchi, A. Ellington, M. Stanton, *Anal. Biochem.* **2001**, *294*, 126 – 131.

